Supplementary Information (SI) for Journal of Materials Chemistry C.
This journal is © The Royal Society of Chemistry 2025

# Low-bandgap oligothiophene-naphthalimide oligomeric semiconductors for organic thermoelectrics.

*Matías J. Alonso-Navarro,[a,b‡], Osnat Zapata-Arteaga,[c‡] Sergi Riera-Galindo,[c] Jiali Guo,[c] Aleksandr Perevedentsev,[c] Edgar Gutiérrez-Fernández,[d] Juan Sebastián Reparaz,[c] Mar Ramos, [b] Christian Müller,[e] Jaime Martín,[d] Marta Mas-Torrent,[c] José L. Segura,[a*] and Mariano Campoy-Quiles.[c*]*

[a]Department of Organic Chemistry, Complutense University of Madrid, Faculty of Chemistry, Madrid 28040, Spain.
[b] Chemical and Environmental Technology Department, Rey Juan Carlos University, Madrid 28933, Spain.

[c]Institut de Ciència de Materials de Barcelona (ICMAB-CSIC), 08193 Bellaterra, Spain.

[d]POLYMAT, University of the Basque Country UPV/EHU Av. de Tolosa 72, 20018,

Donostia-San Sebastián, Spain.

[e] Department of Chemistry and Chemical Engineering Chalmers University of Technology, Göteborg 41296, Sweden.

[‡] Equal contribution

**Table of contents**

## General Information

All the chemicals were purchased from commercial suppliers and used without further purification. **NIP3T** and **NIP3T-Br** compounds were obtained as previously described.[1,2] $^{1}$H-NMR and $^{13}$C-NMR spectra were recorded on a Bruker Avance 300 MHz and AMX 500 spectrometers. Chemical shifts are reported in ppm and referenced to the residual non-deuterated solvent frequencies ($CDCl_3$: δ 7.26 ppm for $^{1}$H, δ 77.0 ppm for $^{13}$C). Solid state $^{13}$C cross-polarization magic angle spinning NMR ($^{13}$C-CP/MAS-NMR) spectra were recorded on a Bruker AVANCE III HD-WB 400 MHz with a rotation frequency of 12 kHz. Mass spectra were recorded on a Bruker Reflex 2 (MALDI-TOF). FTIR spectra were measured with a Shimadzu FTIR 8300 spectrophotometer. The equipment used to carry out thermal analyses is TA Instruments SDTQ600. The atmosphere used during the thermal tests is $N_2$ with a flow rate of 100 mL/min. Material samples were placed in platinum capsules for measurement. The specific test carried out involves a heating ramp from room temperature to 700 $^{o}$C with a heating rate of 10 $^{o}$C/min. SEC of the polymers was performed on an Agilent PL-GPC 220 integrated high-temperature GPC/SEC system in 1,2,4-trichlorobenzene at 150 °C using relative calibration with polystyrene standards. UV–vis absorption spectra of the compounds in HPLC chlorobenzene solutions at 20 $^{o}$C were recorded on a Varian Cary 50 UV–vis spectrophotometer and the thin-film absorption spectra were recorded by drop-casting the solutions onto quartz substrates. Cyclic voltammograms were recorded under inert atmosphere in electrochemical workstation at a scan rate of 100 $mV \cdot s^{-1}$ at 20 $^{o}$C using tetrabutylammonium hexafluorophosphate ($TBAPF_6$, 0.1 mol $L^{-1}$) as supporting electrolyte in chlorobenzene. Polymer-precoated platinum electrode, platinum–wire electrode, and $Ag/Ag^{+}$ electrode were used as working-, auxiliary- and reference electrodes, respectively. Potentials were recorded versus $Fc/Fc^{+}$.

## Synthesis of compounds and characterization

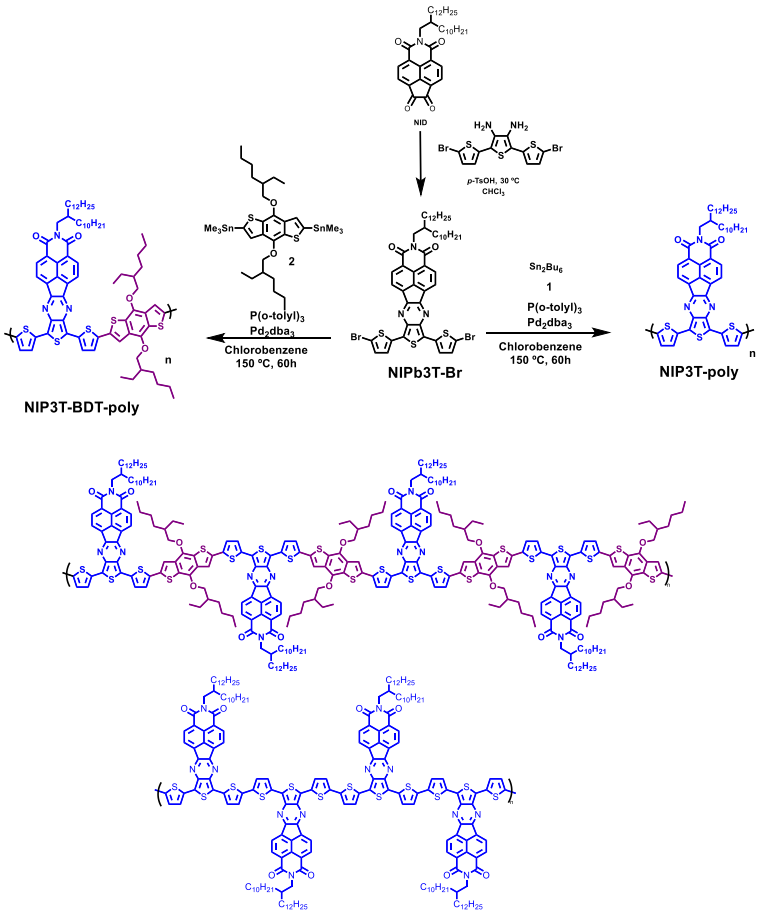


*Scheme S1. Reaction schemes for the synthesis of NIP3T-Br, NIP3T-BDT-poly and NIP3T-poly D-A-D polymers (top) and expanded chemical structures for these π-conjugated materials (bottom).*

**NIP3T-Br:** To a 15 mL anhydrous chloroform solution of NIDb (161 mg, 0,275 mmol), a catalytic amount of p-TsOH (10%) was added and the mixture was stirred for 5 min. After that, an anhydrous chloroform solution of 5,5''-dibromo-[2,2':5',2''-terthiophene]-3',4'-diamine (120 mg, 0.275mmol) was added. The solution turns instantly to a dark blue color, and it was stirred overnight at room temperature. The solvent was evaporated under reduced pressure and the crude was precipitated in MeOH. The solid was filtrated and washed with water, MeOH and hot MeOH to obtain 246mg (72%) of a dark blue solid.

$^{1}$H-NMR (300MHz, 25 $^{o}$C): δ (ppm) = 8.50 (d, J = 8.47 Hz, 2H), 8.10 (d, J = 8.08 Hz, 2H), 6.95 (d, J= 6.97 Hz, 2H), 6.85 (d, J= 6.86 Hz, 2H), 4.1 (m, 2H), 2 (s, 1H), 1.4 (m, 8H), 0.95 (m, 6H).

$^{13}$C-NMR (300MHz, 25 $^{o}$C): δ (ppm) = 163.47, 152.10, 135.91, 135.67, 134.98, 134.65, 131.83, 129.01, 125.72, 123.66, 121.12, 115.96, 77.58, 77.36, 77.16, 76.74, 32.12, 31.90, 30.41, 29.91, 29.87, 29.56, 26.68, 22.87, 14.31.

*General procedure for polymerization reaction via Stille cross-coupling reaction for NIP3T-poly and NIP3T-BDT-poly.*

**NIP3T-Br** and the corresponding distannylated derivative **1** or **2** in stoichiometric 1:1 ratio, P(*o*-tolyl)$_3$ (0.35 eq) and $Pd_2(dba)_3$ were added under Ar atmosphere and dissolved in 5 mL of anhydrous chlorobenzene. Then, the reaction was heated to 140 °C and stirred over 48h. When the reaction time is complete, the crude was cooled down and 0.1 mL of 2-(Tributylstannyl)thiophene were added to the mixture and heated again to 140 $^{o}$C during 1h. The reaction then was cooled, and the crude was poured into 100 mL of MeOH/HCl (10%, 36.5 c/c) solution and stirred 1h. The solid was filtered and wash with water and MeOH and dried and then transferred to a Soxhlet thimble to subject a sequential Soxhlet extraction with MeOH, hexane, dichloromethane, chloroform and finally chlorobenzene. The final fraction was then poured into methanol and the precipitate was filtered and dried to obtain the target polymer in different yields.

**NIP3T-Poly:** The solid was collected and filtrated to obtain a Blueish-black powder (Yield: 65%) $^{1}$H-NMR (300MHz, 25 $^{o}$C): 8.50 (bs, 2H), 8.15 (bs, 2H), 7.35 (bs, 2H), 7.10 (bs, 2H), 4.1 (m, 2H). All the protons left from the alkyl chain could not be possible to integrate. $^{13}$C- CP-MAS-NMR: 165.0 (C=O), 154.2 (C=N), 145.0-110.5 (C=C), 41.2 (C-N), 35.2-10.1 (C-C). FTIR (ATR): υ (cm$^{-1}$): 2958, 2924, 2861, 1698, 1669, 1638, 1588, 1454, 1421, 1326. $M_n$ = 1.27, $M_z$ = 5202, $M_w$ = 11.8 KDa, Đ = 4.1. MALDI-HRMS (m/z) calc. for $C_{50}H_{59}N_3O_2S_3$: 829.38, found ($M^+$): 9123.18.

**NIP3T-BDT-Poly:** The solid was collected and filtrated to obtain a greenish-black powder (Yield: 45%) $^{1}$H-NMR (300MHz, 25 $^{o}$C): 8.50 (bs, 2H), 8.15 (bs, 2H), 7.35 (bs, 2H), 7.10 (bs, 2H), 4.1 (m, 2H). All the protons left from the alkyl chain could not be possible to integrate. $^{13}$C- CP-MAS NMR: 165.0 (C=O), 154.2 (C=N), 145.0-110.5 (C=C), 41.2 (C-N), 35.2-10.1 (C-C). FTIR (ATR): υ (cm$^{-1}$): 2958, 2924, 2861, 1698, 1669, 1638, 1588, 1454, 1421, 1326. $M_n$ = 1.99, $M_z$ = 8.73, $M_w$ = 18.2 KDa, Đ = 4.4. MALDI-HRMS (m/z) calc. for $C_{76}H_{95}N_3O_4S_5$: 1273,59, found ($M^+$): 7641.54.

| Polymer | Reaction | NIP3T-Br (mg) | Temperature (ºC) | Time (h) | MALDI-HRMS (peaks) |
|---|---|---|---|---|---|
| **NIP3T-poly (MA290)** | Carrius tube | 40 | 160 | 16 | 4146.97, 4975.12, 5805.22, 6637.67 |
| **NIP3T-poly (MA291)** | microwave | 45 | 160 | 3.5 | 4145.76, 4971.68, 5799.55, 6630.93, 7456.54, 8280.16 |
| **NIP3T-poly (MA359)** | Carrius tube | 67 | 150 | 72 | 2483.36, 3310.73, 4140,64, 4969.27, 5794.33, 6680.99 |
| **NIP3T-poly (MA442)** | Carrius tube | 120 | 150 | 72 | 4143.09, 4972.37, 5801.90, 6630.16, 7456.10, 8280.78, 9110.57, 9939.18 |
| **NIP3T-BTD-poly (MA361)** | Carrius tube | 84 | 150 | 72 | 2620.42, 3066.56, 3511.46, 3820.06, 4201.44, 4263.62, 5095.37, 5536.93, 6000.31,6814.28, 7718.76 |
| **NIP3T-BTD-poly (MA366)** | Carrius tube | 84 | 150 | 72 | 4805.30, 5633.52, 6909.86, 7351.05, 8177.35 |
| **NIP3T-BTD-poly (MA441)** | Carrius tube | 120 | 150 | 72 | 3896.33, 4413.83, 5245.59, 5610.35, 6437.04, 7418.57, 8309.85, 8980.89. |

Table S1. Reaction conditions scope for the polymerization of **NIP3T-poly**.

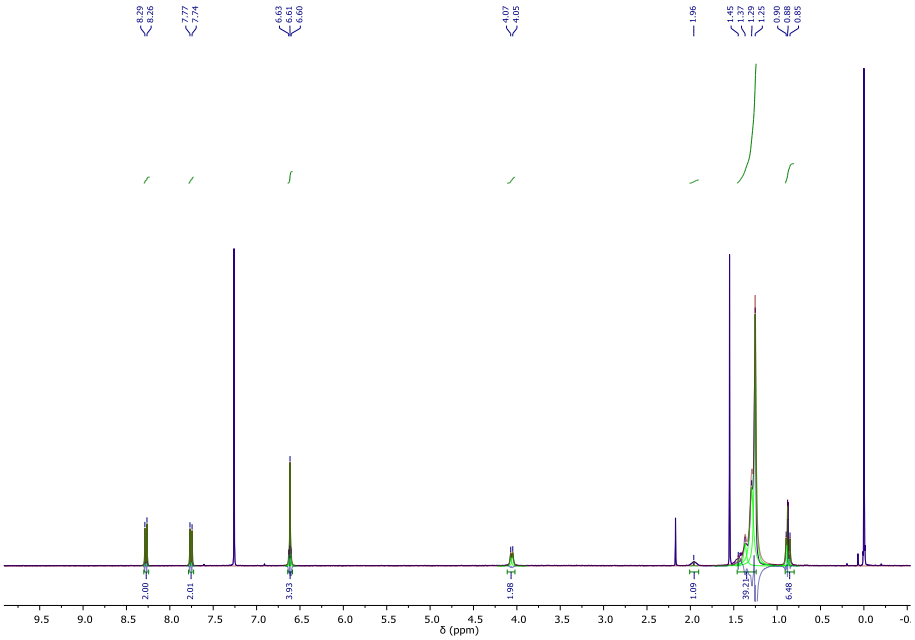


*Figure S1. $^{1}$H-NMR spectrum of NIP3T-Br in $CDCl_3$.*

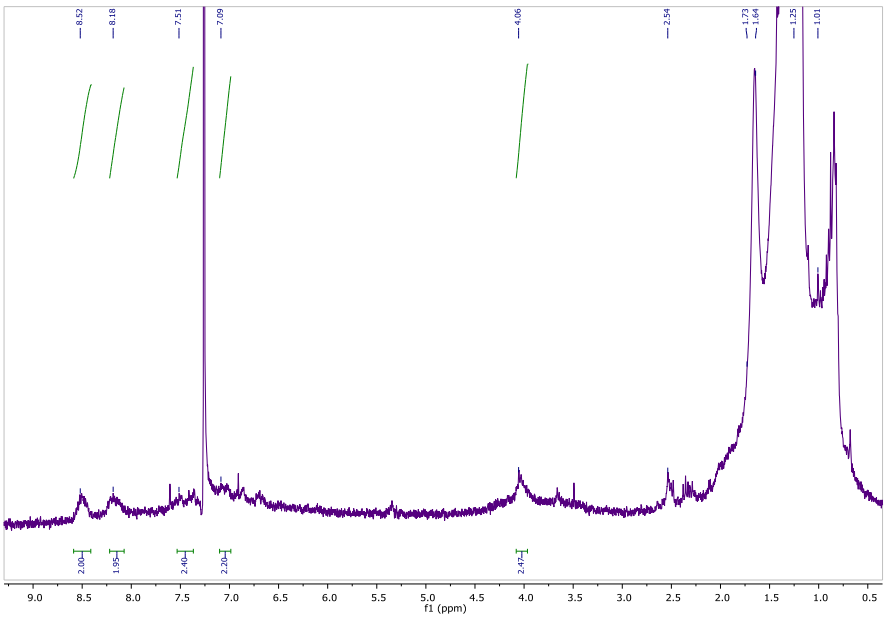


*Figure S2. $^{1}$H-NMR spectrum of NIP3T-poly in $CDCl_3$.*

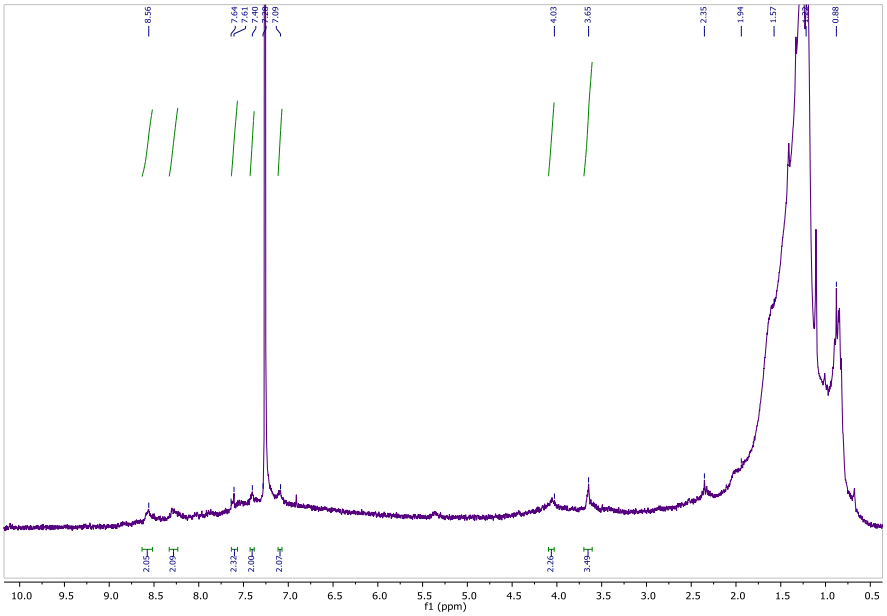


*Figure S3. $^{1}$H-NMR spectrum of NIP3T-BDT-poly in $CDCl_3$.*

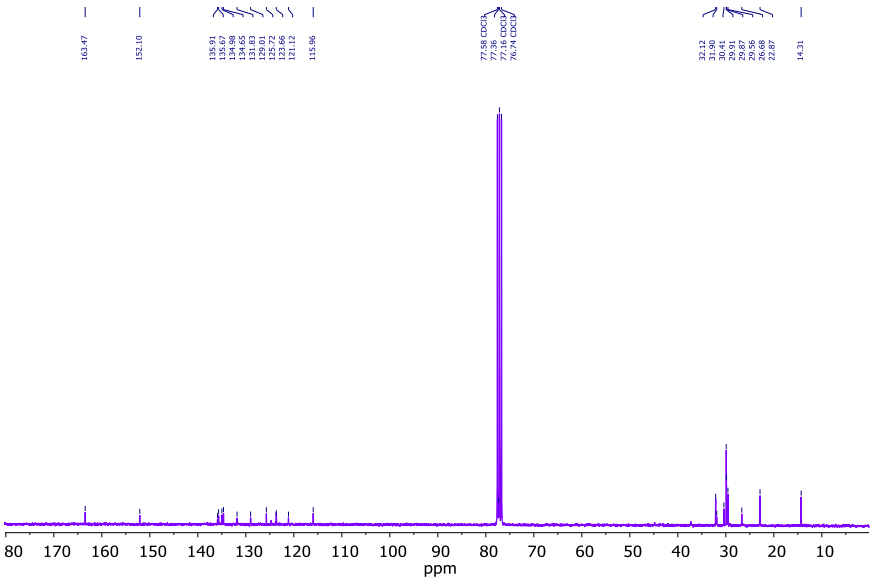


*Figure S4. $^{13}$C-NMR spectrum of NIP3T-2Br in $CDCl_3$.*

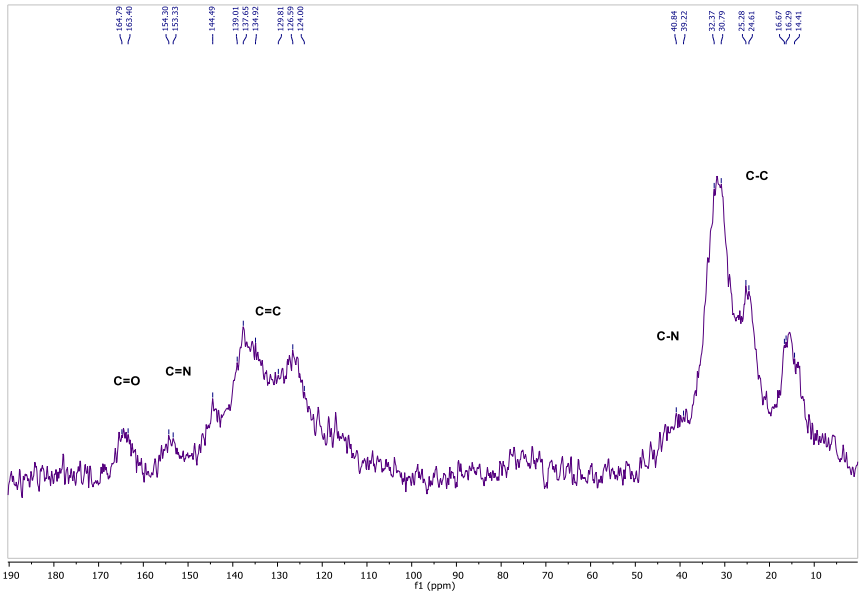


*Figure S5. Solid-state $^{13}$C CP-MAS NMR spectrum of NIP3T-poly.*

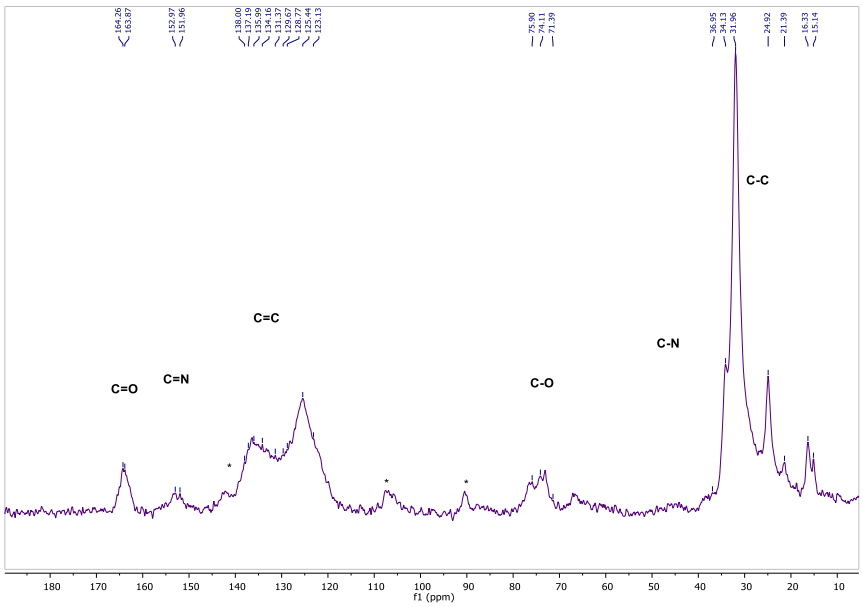


*Figure S6. Solid-state $^{13}C$ CP-MAS NMR spectrum of NIP3T-BDT-poly.*

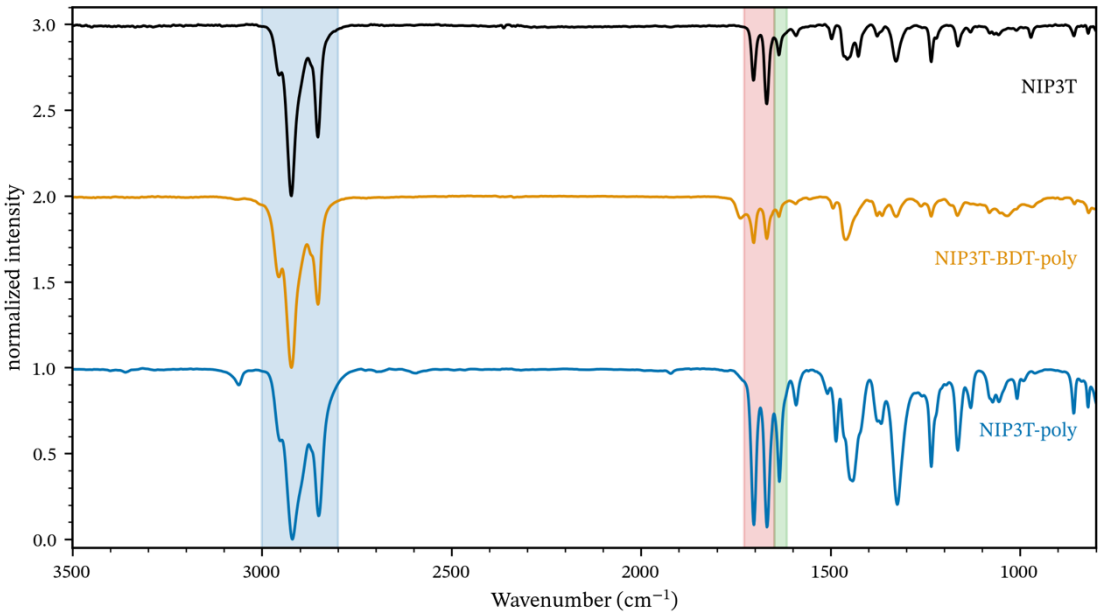


*Figure S7. IR spectra of NIP3T, NIP3T-poly and NIP3T-BDT-poly measured with a diamond plate (ATR). Spectra are offset for clarity. Blue bar indicates CHn, red bar and green bar indicates C=O, C=N stretching modes from the conjugated polymer.*

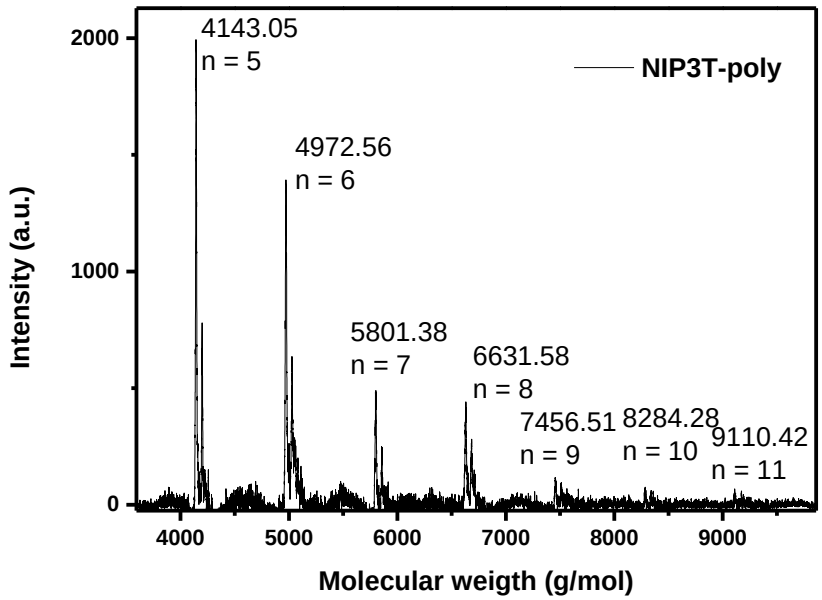


*Figure S8. MALDI-HRMS (m/z) spectrum of NIP3T-poly.*

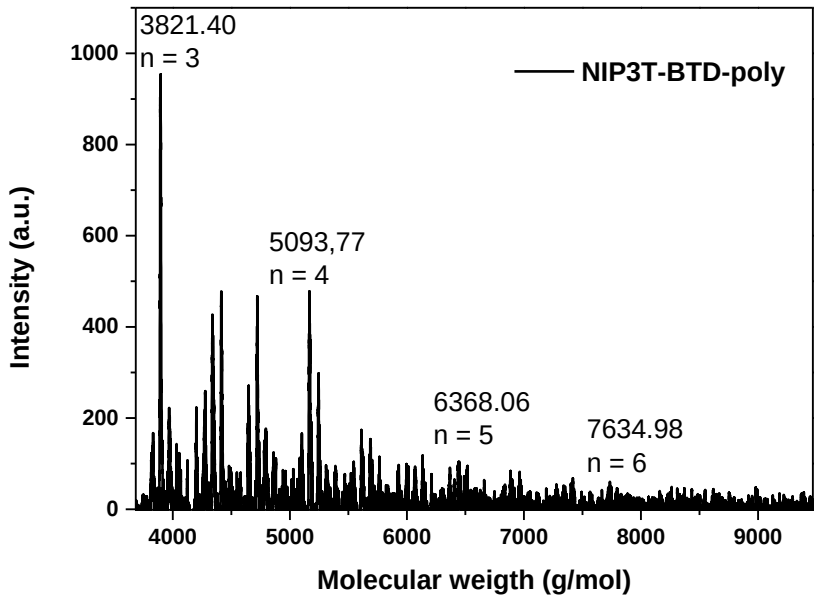


*Figure S9. MALDI-HRMS (m/z) spectrum of NIP3T-BTD-poly.*

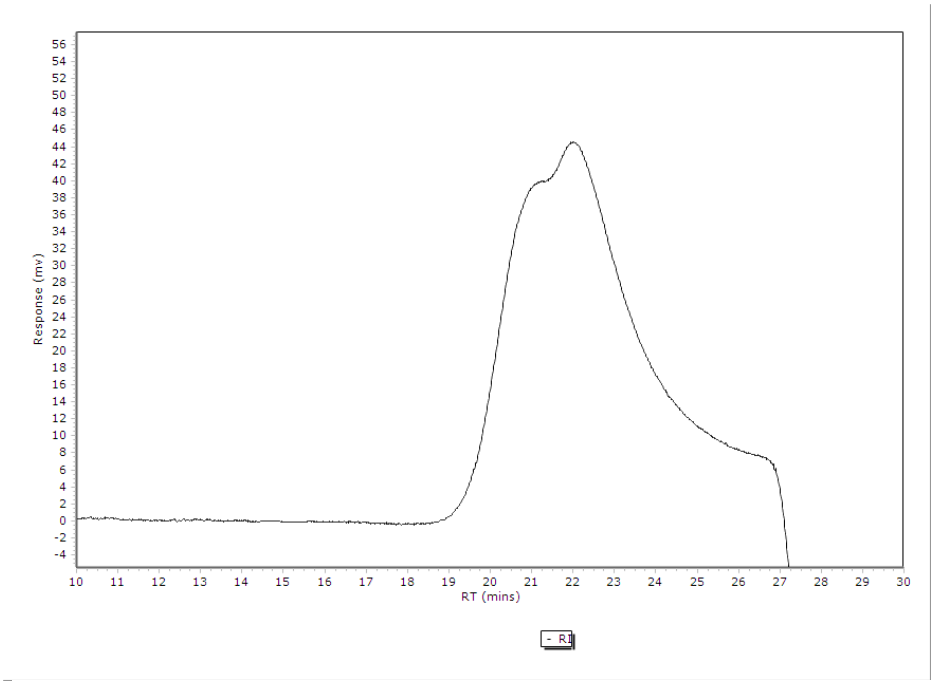


**Molecular Weight Averages**

| Peak | Mp | Mn | Mw | Mz | Mz+1 | Mv | PD |
|---|---|---|---|---|---|---|---|
| Peak 1 | 2679 | 1274 | 5202 | 11848 | 18526 | 10900 | 4,083 |

*Figure S10. GPC trace for NIP3T-poly.*

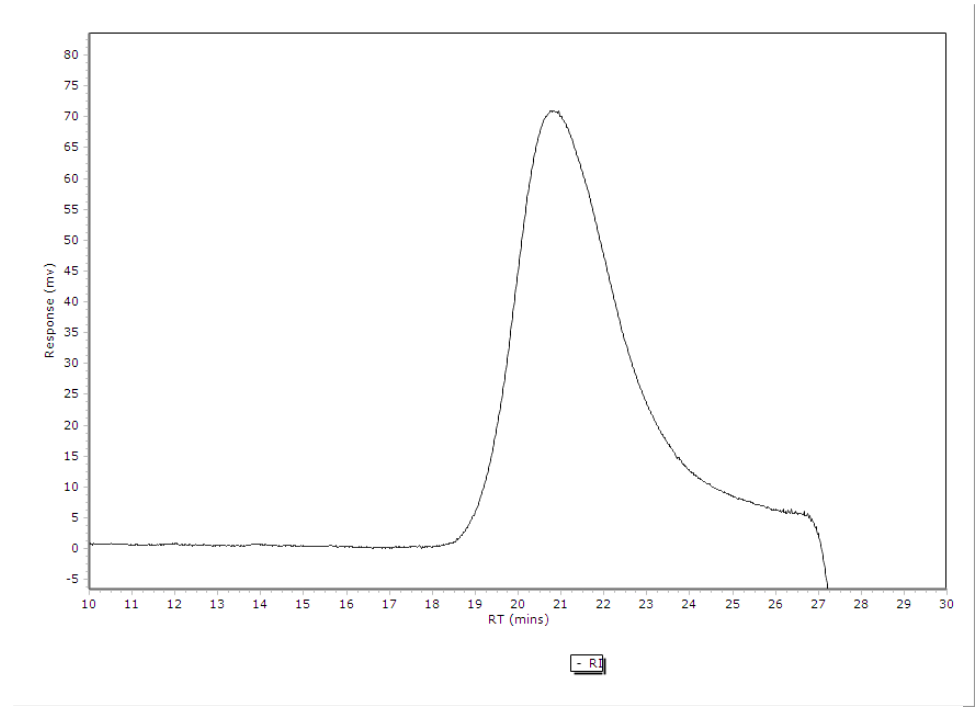


**Molecular Weight Averages**

| Peak | Mp | Mn | Mw | Mz | Mz+1 | Mv | PD |
|---|---|---|---|---|---|---|---|
| Peak 1 | 8852 | 1988 | 8731 | 18228 | 28359 | 16840 | 4,392 |

*Figure S11. GPC trace for NIP3T-BDT-poly.*

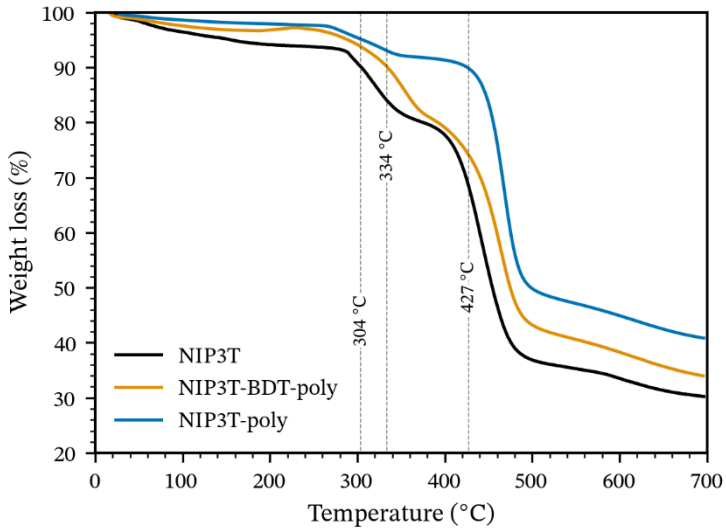


*Figure S12. TGA thermograms for NIP3T (black), NIP3T-poly (blue) and NIP3T-BDT-poly (orange). The respective temperatures corresponding to 10 wt% loss are indicated with arrows.*

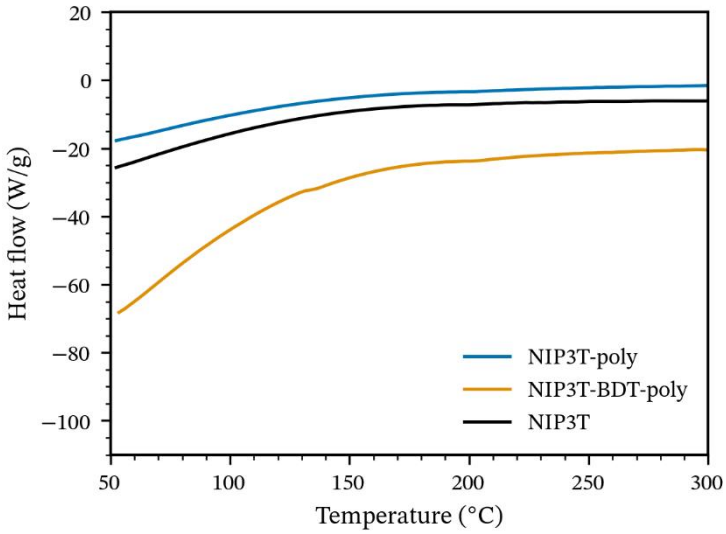


*Figure S13. First-heating DSC thermograms for NIP3T (black), NIP3T-poly (blue) and NIP3T-BDT-poly (orange).*

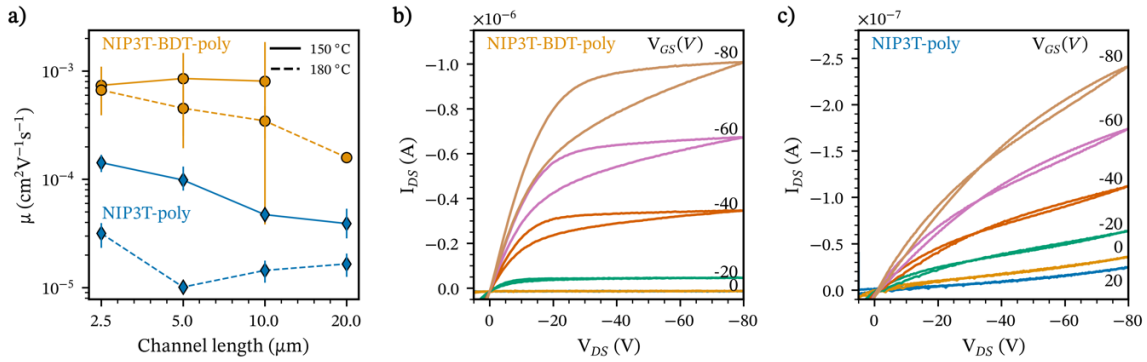


*Figure S14. a) Mobility measurements for NIP3T-poly and NIP3T-BDT-poly for two different annealing temperatures. Output curves for the (b) NIP3T-BDT-poly and (c) NIP3T-poly*

**Optical microscopy**

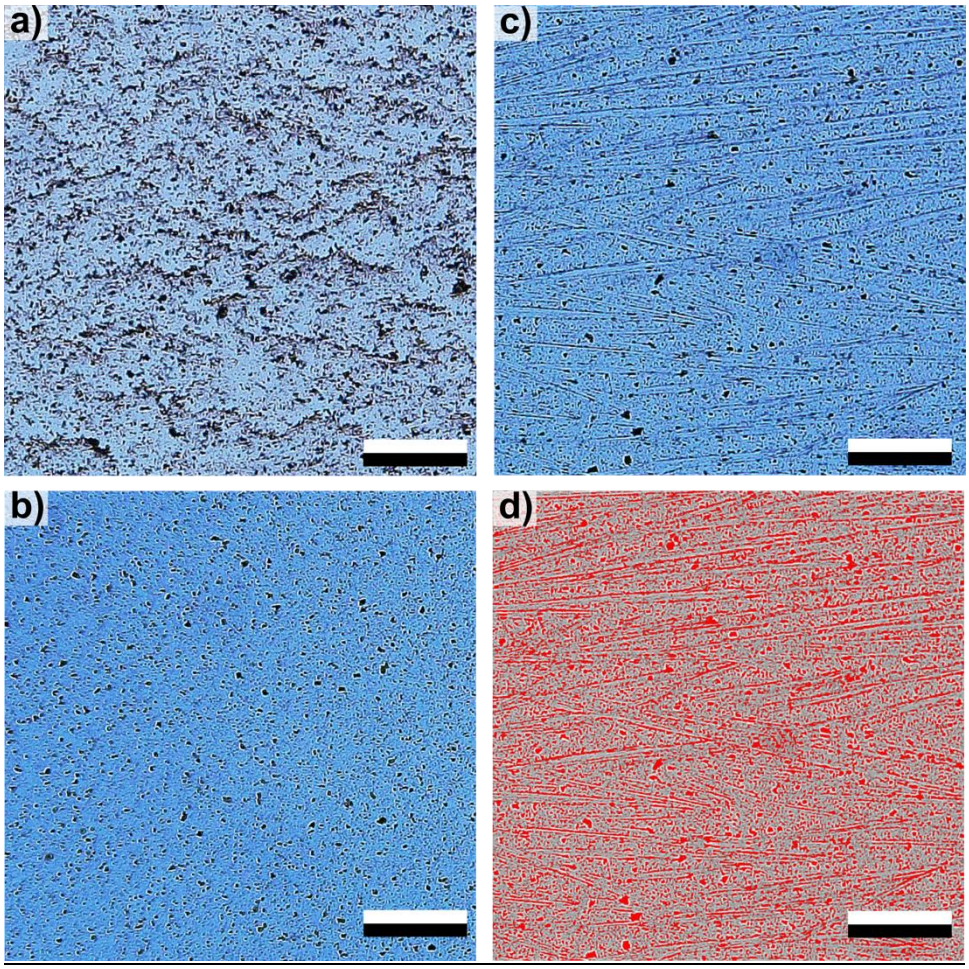


*Figure S15. Transmitted light microscopy images for films of (a) NIP3T-poly and (b) NIP3T-BDT-poly. Both polymers showed a rough surface. For NIP3T-BDT-poly, we evaluated (c) uniaxially oriented polymer films fabricated using small molecule epitaxy. Figure in panel (d) corresponds to a copy of (c) after applying an edge detection filter. The scale bar corresponds to 200 µm.*

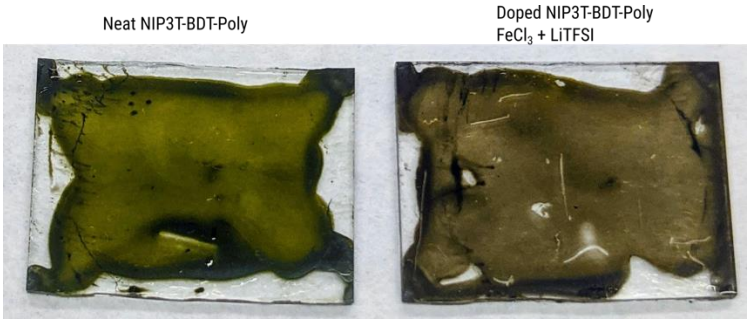


*Figure S16. Photographs of drop-casted NIP3T-BDT-Poly neat and doped. Under the studied blade- coating and spin-coating conditions thin films were mostly transparent to the naked eye. On drop-casted films visual ques between the neat and doped films were more obvious.*

## Electrical and thermal characterization

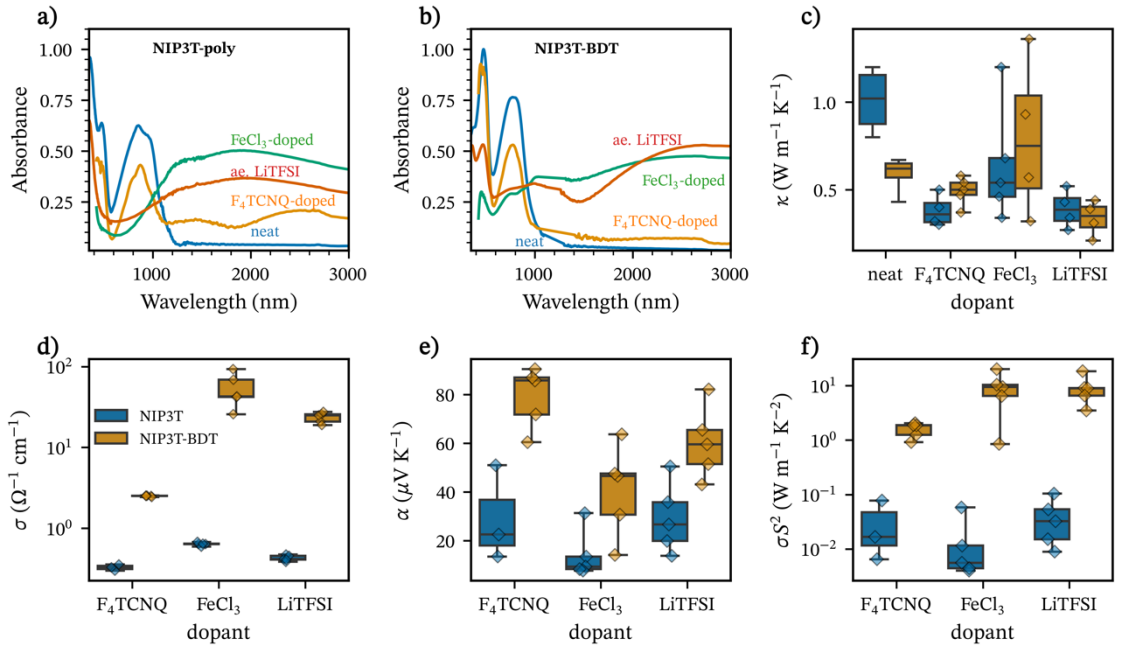


*Figure S17. UV-Vis-NIR spectra of (a) NIP3T-poly and (b) NIP3T-BDT-poly films: neat and doped with three different dopants. ae. LiTFSI, refers to the doped material using FeCl3 and then exchanging the anion with TFSI. c) Thermal conductivity, d) electrical conductivity, e) Seebeck coefficient, and f) power factor. Scatter points are measurements from 4 samples.*

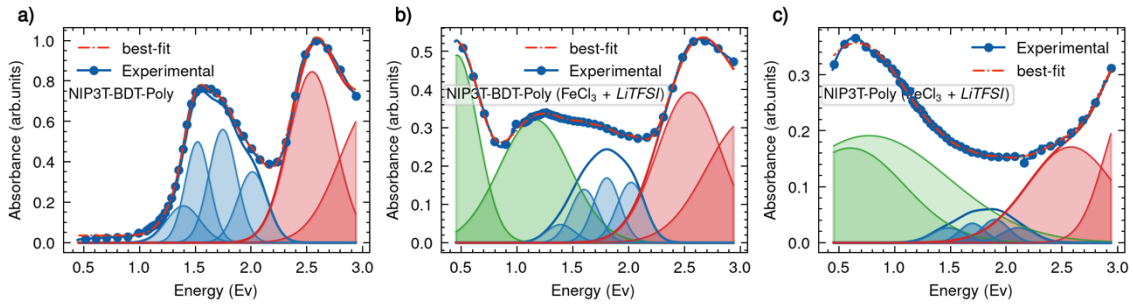


*Figure S18. Spectral analysis: UV-Vis-NIR spectra of neat NIP3T-BDT-Poly and the FeCl3 + LiTFSI anion exchanged NIP3T-Poly and NIP3T-BDT-Poly. Blue and red correspond to the different regions of the neutral polymer, whereas green bands correspond to the polaron P1 and P2 transitions.*

*The polaron mole fraction was estimated according to the work of Moulé et.al.,* [3] *In brief, the the fraction of doped polymer sites are estimated from the ratio of polaron absorbance integra to the total absorbance integral following equation S1:*

$$\Theta = \frac{N_p}{N_p + N_n} = \frac{\int_{0eV}^{4eV} A_p(v)dv - \eta}{\int_{0eV}^{4eV} A_p(v)dv + \int_{0eV}^{4eV} A_n(v)dv}$$

*The model assumes does not distinguish between charge transfer complexes and Integer charge transfer species and includes a correction factor η* that accounts for the increase in total absorbance as doping level increases.

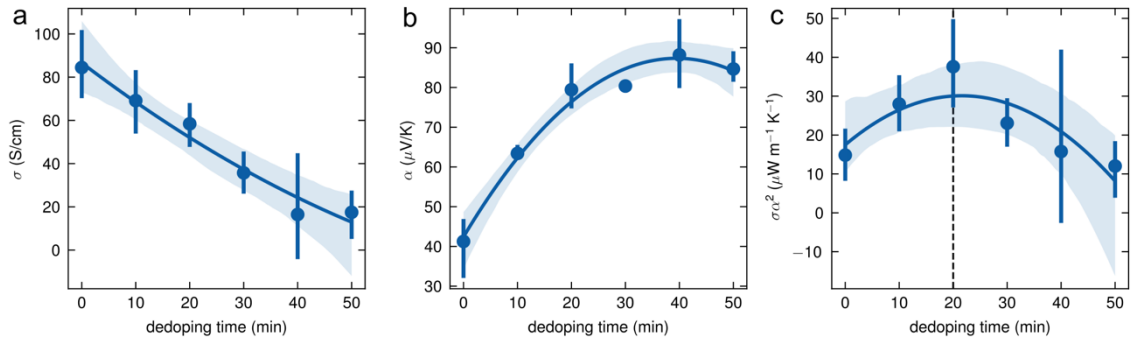


*Figure S19. Optimization of the doping level in anion exchange doped NIP3T-BDT-poly. For the optimization, the films were thermally dedoped on a hotplate at 150 °C in 10 min intervals ambient atmosphere. (a) electrical conductivity, (b) Seebeck coefficient, and (c) power factor.*

**UV-Vis-NIR characterization**

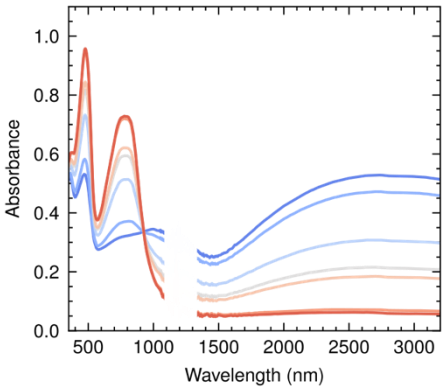


*Figure S20. Optimization of the doping level in anion exchange doped NIP3T-BDT-poly. For the optimization, the films were thermally dedoped on a hotplate at 150 °C in 10 min intervals ambient atmosphere, and the evolution was tracked using UV-Vi-NIR spectra. The missing space corresponds to missing data, as measurements were taken using two different setups.*

## 9. References


1 R. P. Ortiz, H. Herrera, M. J. Mancheño, C. Seoane, J. L. Segura, P. M. Burrezo, J. Casado, J. T. L. Navarrete, A. Facchetti and T. J. Marks, *Chemistry – A European Journal*, 2013, **19**, 12458–12467.

2 M. J. Alonso-Navarro, A. Harbuzaru, P. de Echegaray, I. Arrechea-Marcos, A. Harillo-Baños, A. de la Peña, M. M. Ramos, J. T. L. Navarrete, M. Campoy-Quiles, R. P. Ortiz and J. L. Segura, *Journal of Materials Chemistry C*, 2020, **8**, 15277–15289.

3 A. J. Moulé, G. Gonel, T. L. Murrey, R. Ghosh, J. Saska, N. E. Shevchenko, I. Denti, A. S. Fergerson, R. M. Talbot, N. L. Yacoub, M. Mascal, A. Salleo, F. C. Spano, A. J. Moulé, G. Gonel, A. S. Fergerson [+], R. M. Talbot, N. L. Yacoub, T. L. Murrey, R. Ghosh, F. C. Spano, J. Saska, N. E. Shevchenko, M. Mascal, I. Denti and A. Salleo, *Advanced Electronic Materials*, 2022, **8**, 2100888.